DE GRUYTER Open Geosciences 2020; 12: 1105–1115

Research Article

Shutong Li*, Shixiang Li, Xinping Zhou, Xiaofeng Ma, Ruiliang Guo*, Jiaqiang Zhang, and Junlin Chen

The genesis model of carbonate cementation in the tight oil reservoir: A case of Chang 6 oil layers of the Upper Triassic Yanchang Formation in the western Jiyuan area, Ordos Basin, China

https://doi.org/10.1515/geo-2020-0123
received April 17, 2020; accepted September 21, 2020

Abstract: Carbonate cementation is one of the significant tightness factors in Chang 6 reservoir of the western Jiyuan (WJY) area. Based on the observation of core and thin sections, connecting-well profile analysis as well as carbon and oxygen isotope analysis, it is found that ferrocalcite is the main carbonate cements in the Chang 6 reservoir of the WJY area. The single sand body controls the development of carbonate cements macroscopically. Both carbonate cements and calcite veins hold similar diagenetic conditions: the dissolution of plagioclase is the main calcium source and the de-acidification of organic acids is the main carbon source. The diagenetic stage is identified as the mesogenetic A stage. The sedimentary environment is of low salinity. Accordingly, the development model of carbonate cementation in Chang 6 reservoir is summarized into three types: "eggshell pattern," "cutting pattern," and "favorable reservoir pattern." The development degree of carbonate cementation affects the physical properties of reservoir.

Keywords: carbonate cementation, Yanchang formation, genesis model, Ordos Basin, tight oil reservoir

*** Corresponding author: Shutong Li,** Key Laboratory of Petroleum Resources, Gansu Province. Northwest Institute of Eco-Environment and Resources, Chinese Academy of Sciences, Lanzhou 730000, Gansu, China, e-mail: lishutong1979@163.com
*** Corresponding author: Ruiliang Guo,** Shaanxi Key Laboratory of Petroleum Accumulation Geology, Xi'an Shiyou University, Xi'an 710065, China; School of Earth Sciences and Engineering, Xi'an Shiyou University, Xi'an 710065, China; University of Chinese Academy of Sciences, Beijing 100049, China, e-mail: guoruiliang1991@163.com
Shixiang Li, Xinping Zhou: PetroChina Changqing Oil Field Company, Xi'an 710018, China
Xiaofeng Ma: Key Laboratory of Petroleum Resources, Gansu Province. Northwest Institute of Eco-Environment and Resources, Chinese Academy of Sciences, Lanzhou 730000, Gansu, China
Jiaqiang Zhang, Junlin Chen: Key Laboratory of Petroleum Resources, Gansu Province. Northwest Institute of Eco-Environment and Resources, Chinese Academy of Sciences, Lanzhou 730000, Gansu, China; University of Chinese Academy of Sciences, Beijing 100049, China

1 Introduction

Carbonate cementation is a significant diagenesis type in the clastic reservoir [1–3]. It is the product of the interaction between rock and geological fluid in the diagenesis process under the changes of physical and chemical conditions such as temperature and pressure [1,4–6]. The content, source, and occurrence state of carbonate cements have a great impact on the migration and accumulation of oil and gas, as well as the reservoir physical properties [7–9]. In previous studies, it has been found that the carbonate cementation is generally intense in thin sandstone layers which are adjacent to mudstones, and in the sandstone reservoir near the sandstone/mudstone contacts, which is interpreted that mudstone and/or source rock interlayers as carbon and ion sources transporting Ca^{2+}, Mg^{2+}, and Fe^{2+} to the adjacent sandstone reservoir under the condition of compaction and hydrocarbon generation overpressure [5,6,10–13]. However, the genetic model of carbonate cementation in the tight sandstone reservoir behind this phenomenon is rarely studied and discussed thoroughly and deeply. Carbonate cementation is widely developed in Chang 6 tight oil reservoir in the western Jiyuan area (WJY area hereafter), Ordos Basin, China, which is one of the important factors leading to the reservoir tightness [14–16]. Meanwhile, the high content of carbonate cements is also found in the sandstone layer near the boundary of sandstone and mudstone [17]. Previous relevant studies mainly focused on the distribution and source of carbonate cements in tight sandstone reservoirs, but there is a deficiency in the genesis pattern of carbonate cements and development model of a favorable reservoir [5,6,11–13]. Also, the related studies mainly focused on the impact of diagenesis on the carbonate cementation, while the research on the influence of sedimentation factors on the forming and development pattern of carbonate cements is insufficient. Hence, based on the characteristics of sand body development, the microscopic observation of carbonate cementation, the analysis of carbon and calcium source [18,19], the analysis of paleo-temperature and paleo-salinity [14,20], the exploratory studies have been conducted about the genetic model of carbonate cements in the WJY area to provide a scientific basis for the next step exploration work and reference for the relevant study with similar geological features.

2 Geological setting

Ordos Basin is a typical multi-cycle craton basin with a long-term stable sedimentation process located in central and western China [21–23] (Figure 1a). The inner structure of the basin is relatively simple, while faults and folds are relatively developed in the margin [20]. The WJY area is located in the northwestern Ordos Basin, spanning three first-level tectonic units of West margin thrust belt, Tianhuan Depression, and Shanbei Slop (Figure 1b). The Upper Triassic Yanchang formation is a set of terrigenous clastic rock depositional systems with fluvial and lacustrine facies formed in the process of basin subsidence [24,25]. It can be divided into ten reservoir groups, and Chang 6 is the

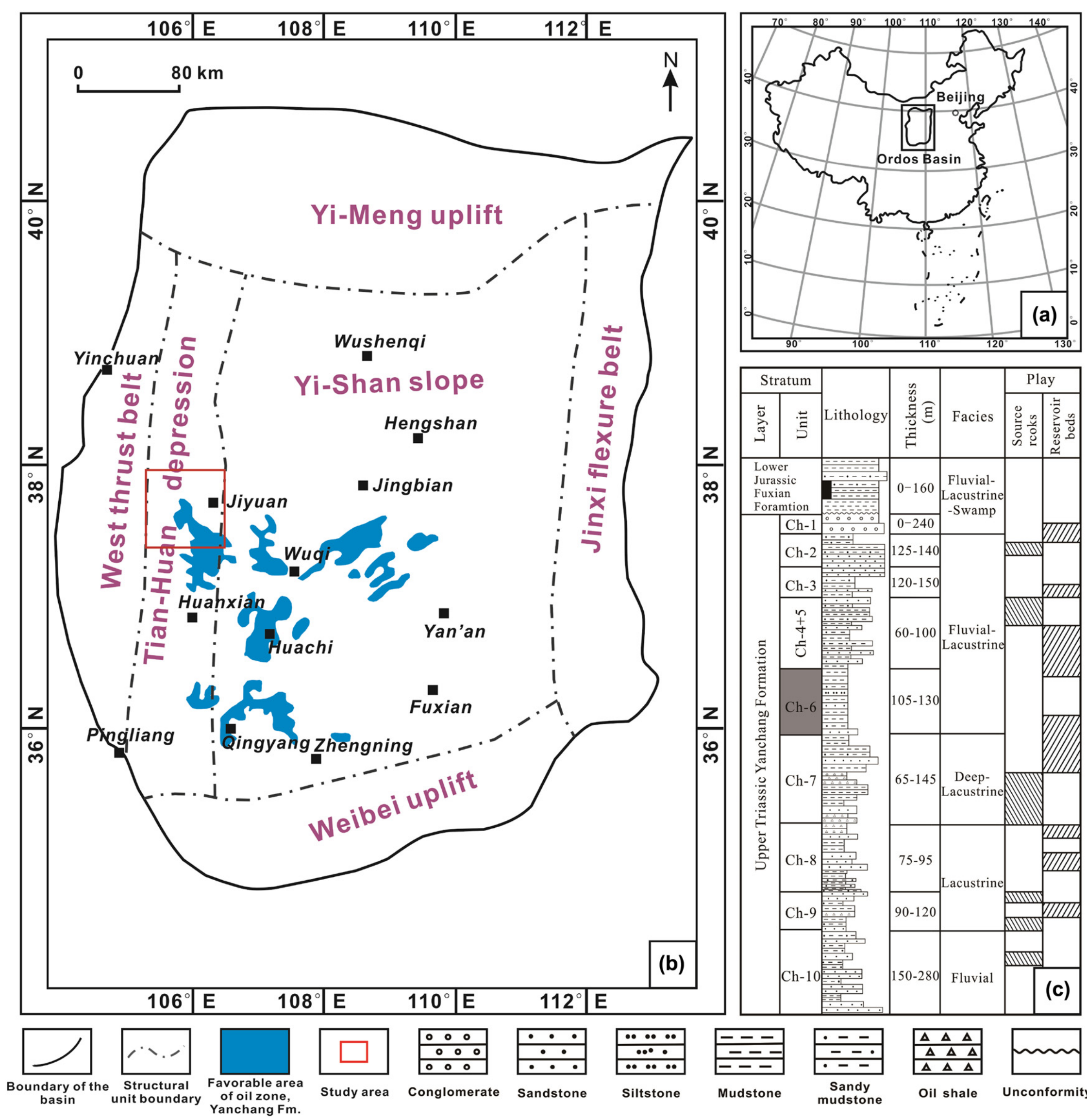

Figure 1: (a) Location of the Ordos Basin in China. (b) Structural division of the Ordos Basin. (c) Lithology section of the Upper Triassic Yanchang Formation in the Ordos Basin, Ch-Chang. Modified after Guo et al. (2020).

first lacustrine recession period after Chang 7 reaches the maximum lacustrine flooding period [26] (Figure 1c). The sediments of Chang 6 in the WJY area are mainly interbedded deposition of fine sandstone, siltstone, pelitic siltstone, and mudstone, which belongs to the delta front sub-facies [14].

3 Samples and methods

First, based on the observation of 115 cores and comprehensive interpretation of 78 single well logging curves, we have established four connecting-well profiles perpendicular to the source supply direction and three profiles parallel to the source supply direction to analyze the sedimentary characteristics of Chang 6 sand body. The well logging curves of Gamma ray and spontaneous potential were used in the profiles to identify reservoir lithology.

Second, utilizing the axioskop 40 polarizing microscope manufactured by Zeiss and the Quanta FEG 450 scanning electron microscope (SEM), 62 samples from 43 wells were collected for microscopic identification in the Key Laboratory of Petroleum Resources Research, Institute of Geology and Geophysics, Chinese Academy of Sciences. By observing 152 thin sections, which were impregnated with blue epoxy resin to highlight the pore spaces and some of them were stained with Alizarin Red S and K-ferricyanide for carbonate mineral identification, we analyzed the reservoir mineral type and content, the degree of sorting and roundness, pore types and diagenesis characteristics. The specific content of diagenetic minerals and cements was quantified by counting at least 350 points of each thin section using an optical collection system. Also, the porosity and permeability data of 237 Chang 6 tight sandstone reservoir samples in WJY area were collected from Changqing Oilfield Company to evaluate the storage and seepage capacity of reservoirs.

In addition, the carbon and oxygen isotopes of 45 sandstone samples and 8 samples of carbonate fillings in fractures were measured in the Key Laboratory of Petroleum Resources Research, Institute of Geology and Geophysics, Chinese Academy of Sciences. The specific process is to conduct the accurate measurement of carbon and oxygen stable isotopes of CO_2 that formed from the dissolution of carbonate materials by H_3PO_4 with MAT-252 isotope mass spectrometer. The measurement accuracy is less than 0.5 ‰, and all isotope data were calibrated with standard samples including NBS-18, GBW04405, and GBW04406. Ultimately, the data were presented relative to the Vienna PeeDee Belemnite (V-PDB) and in the δ notation.

4 Results

4.1 Characteristics of Chang 6 sand body

The sedimentary characteristics of sand body control the physical properties and diagenetic features of the reservoir macroscopically. In this study, four connecting-well profiles perpendicular to the source supply direction and three profiles parallel to the source supply direction were established to analyze the distribution characteristics of Chang 6 sand body in the WJY area. The profiles show that delta front subfacies are mainly developed in Chang 6 tight reservoir of the WJY area, and the delta plain subfacies can be partly found in the northwest of the study area. The underwater distributary channel sand body and the river distributary channel sand body are mainly developed in the delta front sub-facies and delta plain sub-facies, respectively (Figure 2a and b). The river mouth bar is barely developed because of the near-source sedimentary environment [24], where the river carrier is regarded as the “hyper-pycnal flow” relative to lake water and continues to advance toward the lake surface with little lateral diffusion. At the same time, the lake surface is prone to oscillation because of the strong hydrodynamic force [24], and the bottom of the lake basin in the WJY area is relatively gentle [14]. Therefore, the sand body is vertically discontinuous and is separated by a large number of clay interlayers (Figure 2a and b). The deposit thickness of the single-layer sand body is relatively thin and heterogeneous (mainly 2–15 m). In addition, the sand body has good plane continuity and obvious progradation process characteristics (Figure 2a and b). The underwater distributary channel sand body of multiphase superposition vertically can be seen in some wells (Figure 2b), which is formed under the condition of sufficient material supply and depositional accommodation.

On the whole, the slowly progradational underwater distributary channel sand body with good plane continuity and poor vertical continuity was formed in Chang 6 tight sandstone of the WJY area. These features of the sand body will affect the genesis model of carbonate cementation.

4.2 Characteristics of carbonate cement

Through the observation of drilling cores, it can be seen that the calcite veins in Chang 6 tight sandstone

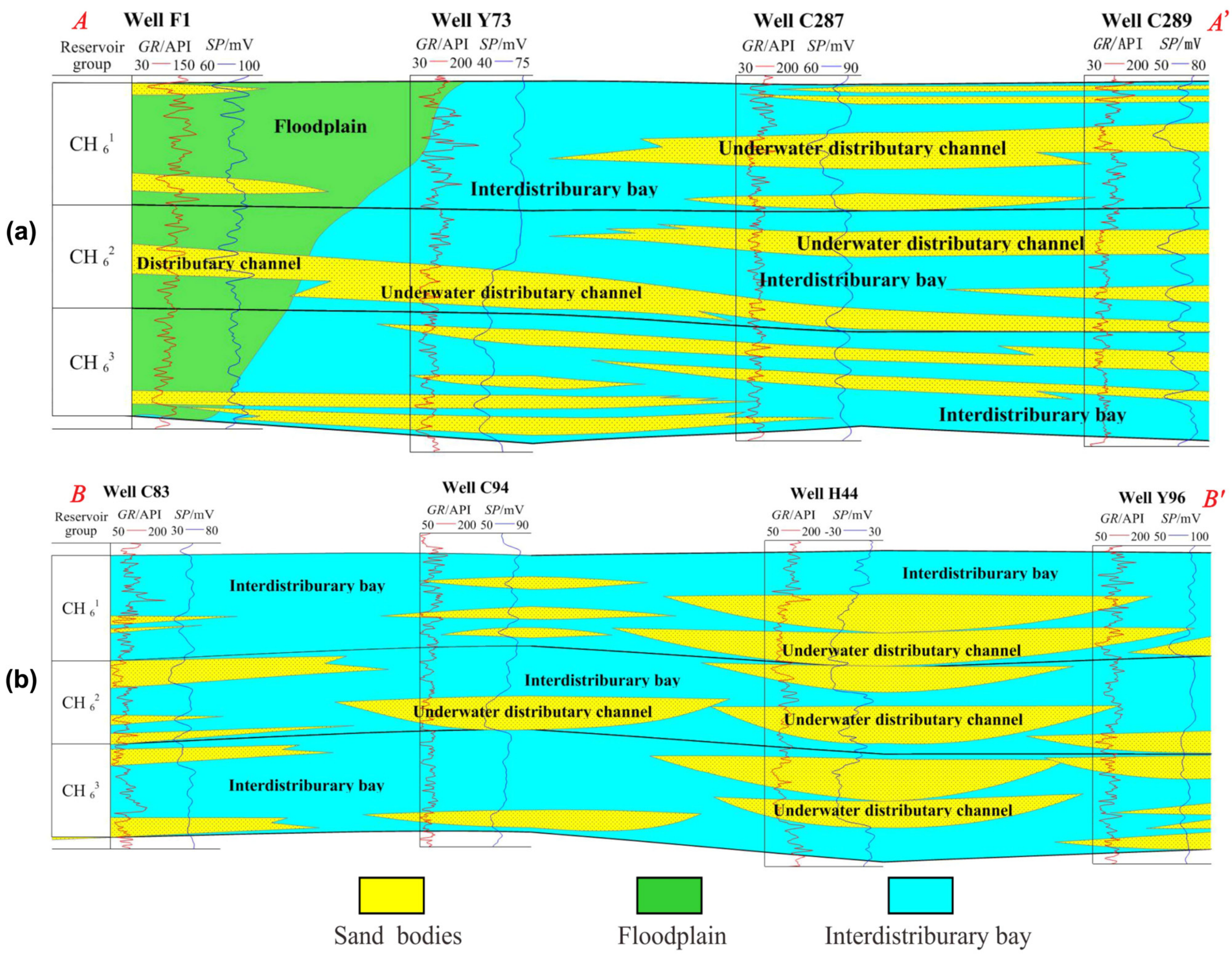

Figure 2: The typical connecting-well profiles of Chang 6 sand body in the WJY area of the Ordos Basin. (a) Profile of well F1-C289 perpendicular to the source supply direction; (b) profile of well C83-Y96 parallel to the source supply direction.

reservoirs of the WJY area are extensively developed (Figure 3a–e). Meanwhile, the development of calcite veins is accompanied by the development of fractures, which is caused by the instability of geological conditions in the West Margin Thrust Belt. In addition, the calcite veins are more developed in the thin sandstones layers adjacent to mudstone.

Based on the observation of 152 thin sections, we can learn that the interstitial materials of Chang 6 reservoirs in the WJY area are mainly cements of carbonate, chlorite, kaolinite, silica, and a small amount of illite. The carbonate cements are the main type and account for about 4.10%. Ferrocalcite is the main form of carbonate cements, which presents deep red to purplish-red after stained with Alizarin Red S (Figure 4a–d), mostly idiomorphic (Figure 4e) or metasomatic feldspar grains (Figure 4f) under the SEM observation, and shows red orange to dark red under the cathode luminescence (CL) (Figure 4g–i). According to the collected porosity data and the counting statistical carbonate cements content of thin sections, it can be seen that carbonate cements have a destructive effect on reservoir physical properties and has a negative correlation with porosity (Figure 5). In addition, ferrocalcite is mainly filled in the intergranular pores between sandstone clastic grains in the form of porphyritic and crystal stock (Figure 4a–d). It even shows the form of semibasement, when the content of carbonate cementation is intense (Figure 4b).

Early carbonate cements are not found in this study. The possible reason is that the early carbonate cements may be replaced by late-stage calcite [27]. Even if there are remnants of early carbonate cements, they cannot be found in stained thin sections due to their extremely low content and heterogeneity.

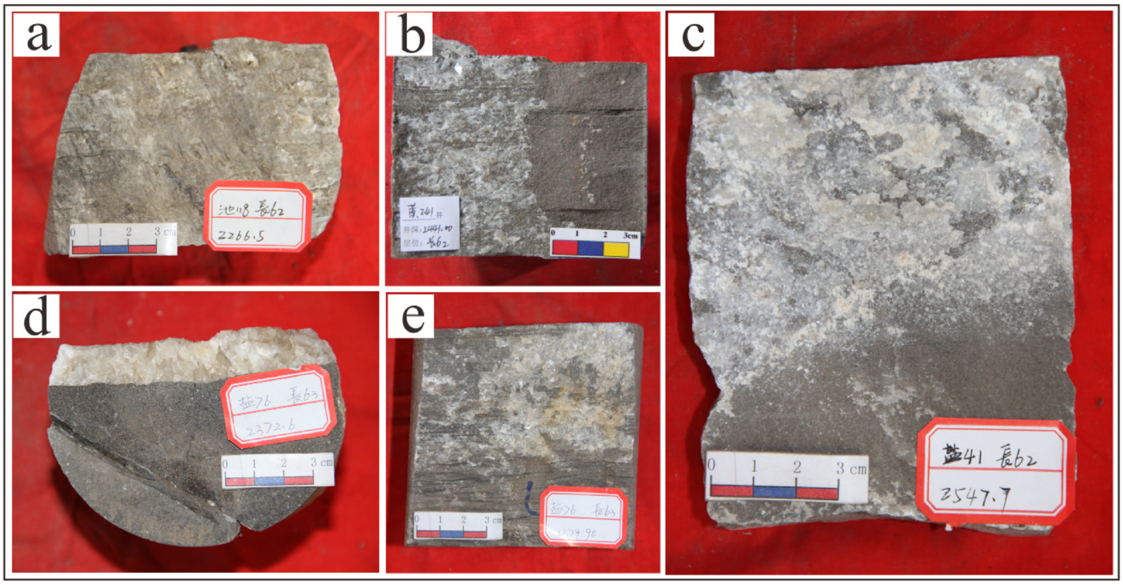

Figure 3: The calcite veins of drilling cores in Chang 6 tight sandstone reservoirs. (a) Well Ch118, 2266.5 m; (b) Well H241, 2441.0 m; (c) Well Y41, 2547.7 m; (d) Well Y76, 2372.6 m; (e) Well Y76, 2379.90 m.

5 Discussion

5.1 Genetic analysis of carbonate cement

5.1.1 Carbon source and calcium source

The genesis analysis of carbonate cementation mainly includes the clarification of carbon source and calcium source. According to the results of previous studies and the sedimentary characteristics of the study area [5,11–14,27], it is concluded that the calcium source of Chang 6 carbonate cementation in the WJY area mainly includes the following aspects. First, the dissolution of feldspar (mainly plagioclase) is a significant calcium source for carbonate cementation. The Ca^{2+} provided by this process (equation (1)) enters into the pore fluid medium to form carbonate cementite, which is one of the mechanisms for the formation of carbonate cements in clastic rocks and is the most important calcium source in the WJY area [28]. Then, the montmorillonite can provide calcium source during the transformation from illite smectite mixed layer (I/S) to illite. Longstaff et al. (1981) proposed the reaction involved in this conversion process, as shown in equation (2) [29]. In addition, the dissolution of carbonate debris and early carbonate cements can provide the calcium source for the carbonate cements formation of the middle and late stage [10].

$$CaAl_2Si_2O_8\ (\text{Anorthite}) \rightarrow Al_2Si_2O_5(OH)_4(\text{Kaolinite}) + Ca^{2+} \quad (1)$$

$$4.5K^{+} + 8Al^{3+} + \text{Smectite} \rightarrow \text{Illite} + Na^{+} + 2Ca^{2+} + 2.5Fe^{3+} + 2Mg^{2+} + 3Si^{4+} \quad (2)$$

To further clarify the formation process, carbon source, and genesis of carbonate cements in Chang 6 reservoirs, the carbon and oxygen stable isotopes of 45 sandstone samples and 8 samples of calcite veins in fractures are measured. The analysis results are shown in Tables 1 and 2. Based on the carbonate genesis identification chart proposed by Curtis in 1977 [18], the carbon and oxygen isotope values of measured samples are set into different zones (Figure 6). The result shows that most of the sample points are distributed in zone III, which is related to the organic matter decarboxylation [30]. A small number of points are distributed in zone II, which is related to the biogas generated by the methane bacteria fermentation [30]. No points are distributed in zone I, which indicates the "diagenetic carbonate cements" associated with sulfate reduction during shallow burial [30]. Significantly, both calcite veins in fractures and carbonate cements have similar distribution characteristics of the carbon and oxygen isotopes.

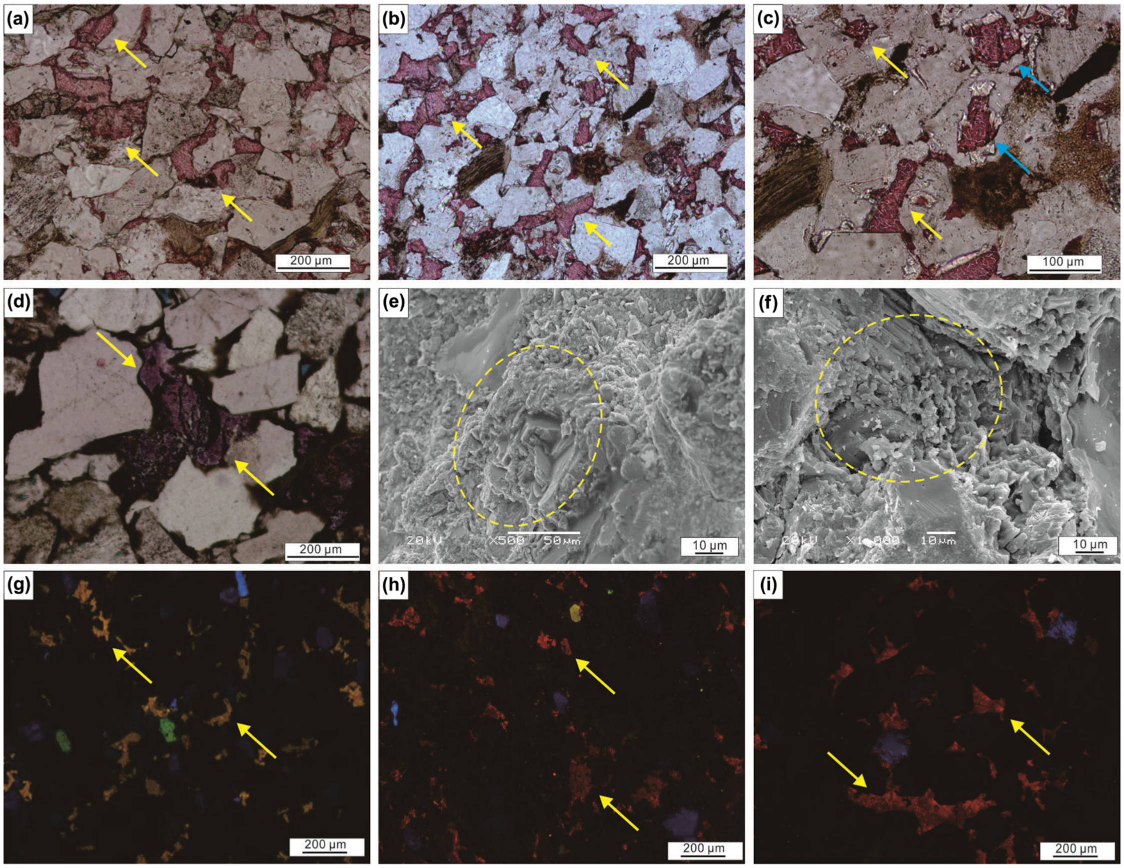

Figure 4: Photomicrographs displaying the characteristics of carbonate cementation of the Chang 6 tight sandstone reservoirs in the WJY area, Ordos Basin. (a) Middle ferrocalcite cements occupies intergranular pore space (yellow arrow), Well H319, 2856.38 m, plane-polarized light (PPL); (b) middle ferrocalcite cements occupies intergranular pore space (yellow arrow), Well H315, 2570.85 m, PPL; (c) middle ferrocalcite cements occupy intergranular (yellow arrow) and intragranular (blue arrow) pore space, Well H315, 2580.75 m, PPL; (d) late ferrocalcite cements metasomatism middle carbonate cements and occupy intergranular pore space (yellow arrow), Well Y83, 2492.42 m, PPL; (e) SEM image of carbonate cements on grain surface (yellow circle), well F11, 2441.56 m; (f) SEM image of carbonate cements slightly dissolved (yellow circle), Well Y73, 2634.12 m; (g) red orange ferruginous calcite cements filling intergranular pore space (yellow arrow), Well H44, 2514.13 m, cathode luminescence (CL); (h) dark red ferrocalcite cements (yellow arrow), Well Y96, 2435.17 m, CL; (i) dark red ferrocalcite cements are well developed and occupy the intergranular pore space (yellow arrow), Well C83, 2483.12 m, CL.

5.1.2 Paleo-temperature of sedimentary environment

Geological fluids temperature is an important factor to control the stable isotopic composition of carbonate. The value of $\delta^{18}O$ is usually used to calculate paleo-temperature and as a geological thermometer for determining ambient temperatures, which can evaluate the environmental conditions and diagenetic stages of cementation. In this study, the mature theoretical equation for geological thermometers which is proposed by Shackleton (1975) is used to calculate the paleo-temperature (T) [31]. The paleo-temperature is actually the forming temperature of carbonate cements, and it is calculated using the following equation:

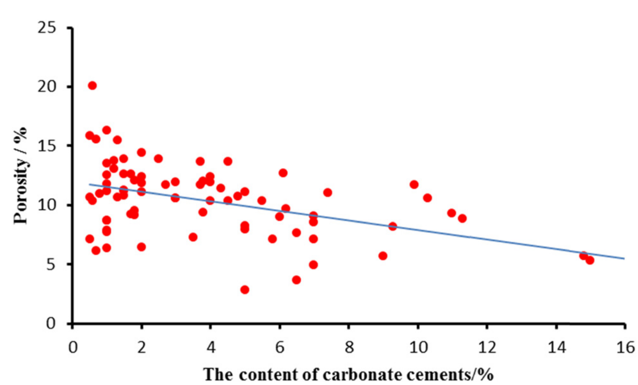

Figure 5: Cross plots of the content of carbonate cements vs porosity of Chang 6 tight sandstone in the WJY area of Ordos Basin.

Table 1: Carbon and oxygen isotopic data of Chang 6 carbonate cements in the WJY area

No.	Well name	Depth/m	$\delta^{13}C_{PDB}$/‰	$\delta^{18}O_{PDB}$/‰	Value of *Z*	Paleotemperature/°C
1	C118	2266.5	−1.913	−21.547	112.65	101.78
2	C18	2153.9	−0.788	−20.972	115.24	97.62
3	C18	2145.5	1.09	−15.022	122.05	58.47
4	C18	2184.86	−0.449	−20.594	116.12	94.92
5	F10	2216.9	−0.763	−22.221	114.67	106.74
6	H132	2336.15	−1.909	−19.55	113.65	87.62
7	H132	2368.25	1.361	−20.877	119.69	96.94
8	H269	2385.8	−1.05	−18.512	115.93	80.58
9	H269	2396.3	0.325	−21.48	117.27	101.29
10	H269	2366	−0.989	−22.307	114.17	107.38
11	H269	2408.7	−0.289	−23.109	115.2	113.41
12	H269	2419.27	0.204	−20.341	117.59	93.13
13	H48	2480.1	−0.84	−21.819	114.71	103.77
14	H83	2455.7	−1.674	−20.687	113.57	95.58
15	H83	2662	−8.742	−21.48	98.7	101.29
16	Y114	2273.6	−2.202	−21.161	112.25	98.98
17	Y115	2298.3	0.184	−14.506	120.45	55.41
18	Y115	2313.8	0.399	−14.511	120.89	55.44
19	Y115	2382.05	−2.428	−18.963	112.88	83.61
20	Y117	2349.4	−1.751	−19.647	113.93	88.29
21	Y117	2351.2	−1.348	−14.11	117.51	53.1
22	Y117	2353.7	−1.422	−17.021	115.91	70.83
23	Y123	2376.1	−3.806	−21.038	109.03	98.09
24	Y28	2440.8	−1.995	−21.482	112.52	101.3
25	Y28	2443.1	−1.262	−22.351	113.58	107.7
26	Y28	2448.28	−2.138	−21.219	112.35	99.4
27	Y41	2506.8	−1.787	−17.555	114.9	74.27
28	Y41	2508.3	−0.473	−15.095	118.81	58.91
29	Y41	2547.7	−4.491	−21.982	107.16	104.97
30	Y41	2556.65	−3.48	−21.208	109.61	99.32
31	Y41	2571.4	−2.566	−22.008	111.08	105.16
32	Y71	2370.1	−1.67	−19.746	114.05	88.97
33	Y71	2415.9	−0.157	−20.799	116.62	96.38
34	Y73	2375.3	0.056	−20.652	117.13	95.33
35	Y76	2345.7	−0.27	−25.53	114.03	132.4
36	Y76	2337.7	−0.312	−23.855	114.78	119.13
37	Y76	2339.7	−0.141	−24.115	115	121.16
38	Y76	2385.62	2.317	−24.793	119.7	126.49
39	Y76	2385.62	−1.218	−20.397	114.65	93.53
40	Y76	2378.95	−0.224	−21.617	116.08	102.29
41	Y76	2372.6	2.127	−24.298	119.56	122.59
42	Y76	2378.95	2.031	−24.221	119.4	121.98
43	Y76	2379.9	0.147	−20.962	117.16	97.55
44	Y76	2385.8	−0.769	−21.365	115.09	100.45
45	Y76	2393.6	−3.002	−19.711	111.34	88.73

$$T(°C) = 16.9 - 4.38 \times (\delta^{18}O - \delta^{18}O_w) + 0.1 \times (\delta^{18}O - \delta^{18}O_w)^2 \quad (3)$$

where the $\delta^{18}O$ uses the PDB standard, $\delta^{18}O_w$ is the oxygen isotope values of geological fluids medium at the time carbonate cements formed, and the value of $\delta^{18}O_w$ is selected as −2.5‰ according to the overall geological environment at the time of the Chang 6 diagenesis period.

The calculation results show that the paleo-temperature of carbonate cements in the Chang 6 reservoirs is ranged from 95 to 110°C (Table 1 and Figure 7). The paleo-temperature of carbonate veins in fractures is distributed in the range of 110–125°C (Table 2 and Figure 7).

Table 2: Carbon and oxygen isotopic data of Chang 6 calcite veins in the WJY area

No.	Well name	Depth/m	$\delta^{13}C_{PDB}$/‰	$\delta^{18}O_{PDB}$/‰	Value of *Z*	Paleotemperature/°C
1	C118	2266.5	−1.484	−18.357	115.12	79.54
2	H241	2441	2.334	−25.766	119.25	134.31
3	Y41	2547.7	0.109	−22.532	116.3	109.05
4	Y76	2372.6	2.046	−24.391	119.34	123.32
5	Y76	2378.95	−0.206	−24.067	114.89	120.78
6	Y76	2379.9	1.038	−23.215	117.86	114.21
7	Y76	2385.62	2.474	−24.434	120.2	123.66
8	Y168	2296.98	−0.218	−18.965	117.41	83.62

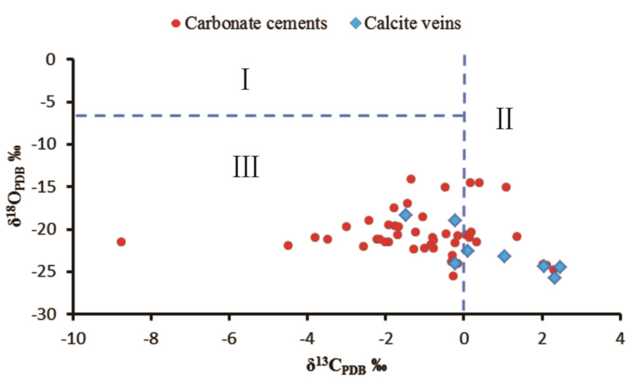

Figure 6: Cross plots of the $\delta^{13}C_{PDB}$ vs $\delta^{18}O_{PDB}$ of carbonate cements and calcite veins of Chang 6 tight sandstone reservoirs in the WJY area, Ordos Basin. The identification map is from Curtis, 1977. (I) The carbonate related to sulfate; (II) the carbonate related to bacteria fermentation; (III) the carbonate related to organic matter decarboxylation.

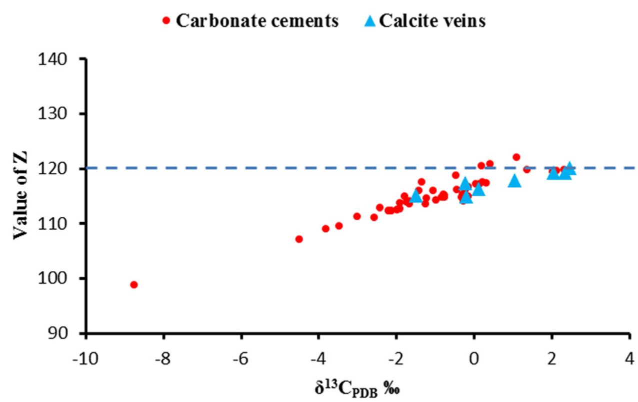

Figure 8: The distribution characteristics of *Z* values of Chang 6 tight sandstone reservoir carbonate cements and calcite veins.

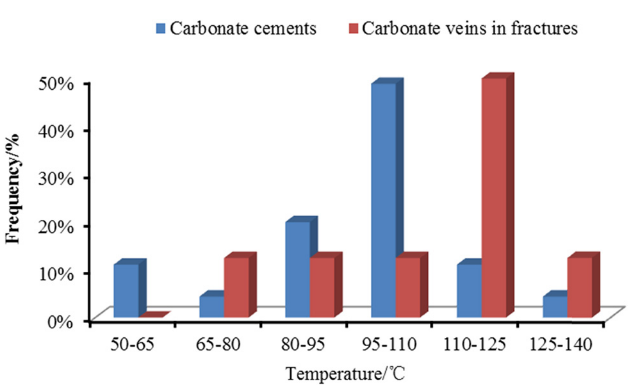

Figure 7: The frequency distribution histogram of paleo-temperature of the Chang 6 tight sandstone reservoir carbonates cements and veins in fracture.

According to the China Petroleum Standard of the Division of Diagenetic Stage in Clastic Rocks (SY/T 5477-2003), the formation temperature of both the carbonate cements and veins in fractures belongs to the Mesogenetic A stage.

5.1.3 Paleo-salinity of sedimentary environment

In the diagenetic process, the salinity of the fluids medium affects the value of $\delta^{18}O$ and $\delta^{13}C$ to a great extent, the isotope values of which generally increases with the increasing of the fluids salinity. In this study, the empirical equation proposed by Keith and Weber (1964) is used to calculate the paleo-salinity (*Z*) of the geological fluids at the time carbonate cements formed [32]. The equation is as equation (4) which can distinguish the carbonate rocks forming condition from marine and freshwater conditions by carbon and oxygen isotope values.

$$Z = 2.048 \times (\delta^{13}C + 50) + 0.498 \times (\delta^{18}O + 50) \quad (4)$$

where the $\delta^{13}C$ and $\delta^{18}O$ use the PDB standard.

It is identified as marine-saline lacustrine facies limestone when $Z > 120$, and is fresh-water limestone when $Z < 120$. The calculation results of *Z* values are shown in Tables 1 and 2 and Figure 8. The *Z* values of all the samples are less than 120 (except for three points slightly higher than 120), which indicates that the sedimentary environment has a

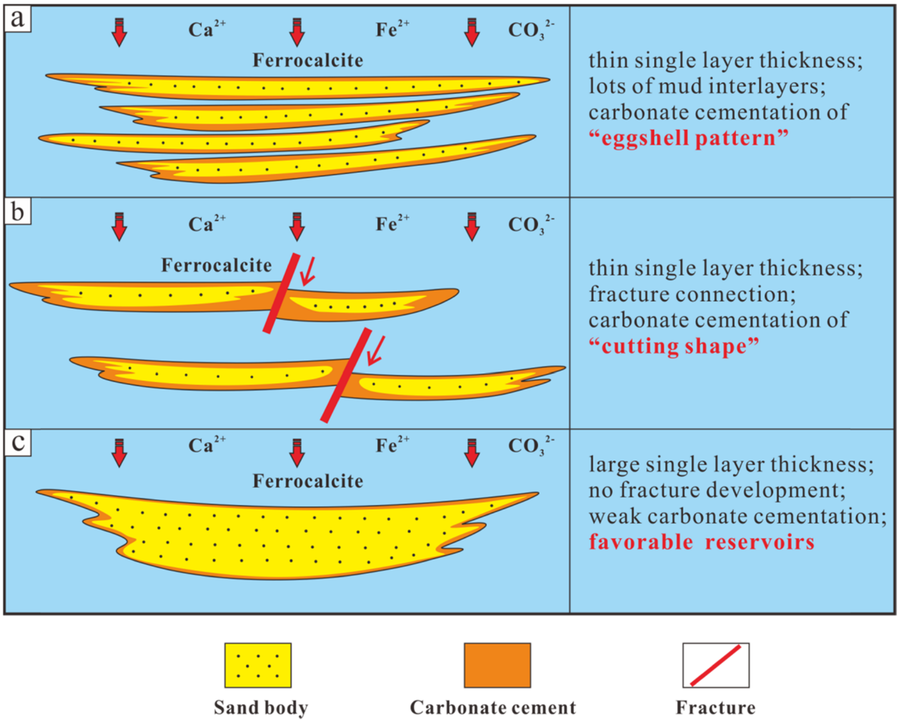

Figure 9: The genesis models of carbonate cementation in Chang 6 reservoir of WJY area. (a) developmental mechanism of "eggshell pattern" carbonate cementation; (b) developmental mechanism of "cutting shape" carbonate cementation; (c) developmental mechanism of the favorable reservoirs.

low salinity, and the carbonate cements as well as calcite veins are formed in the depositional conditions of freshwater and brackish water.

5.2 The genesis model of carbonate cementation

Through the above discussion, it can be seen that both carbonate cements and calcite veins are in the same diagenetic stage and have the same paleo-salinity environment. Meanwhile, the geneses of two types of carbonate samples are mainly related to the de-acidification of organic acids, which are controlled by the development of organic matter to a great extent. Also, the characteristics of Chang 6 sand body indicate that the mudstone interlayers are largely developed between thin sand bodies, with many fractures accompanied. Therefore, sand body thickness, mudstone interlayers, and the development of fractures dominate the development degree of carbonate cements in Chang 6 reservoirs.

Considering the distribution of sand body, the development of mudstone interbeds, and fractures in Chang 6 tight sandstone reservoirs, this study divides the development patterns of carbonate cementation into three types (Figure 9). The first type is called "eggshell pattern," which holds the characteristics of the development of thin single layers sand body and lots of mudstone interlayers (Figure 9a). A large amount of mudstones strengthen the de-acidification of organic acids to provide abundant CO_3^{2-}. Therefore, at the top and bottom of a thin sand body (namely, the surface of eggshell), carbonate cementation is strong and intense. The second type is called "cutting pattern," which holds the features of thin single layers sand body and lots of mudstone interlayers with fractures connected (Figure 9b). The fracture enhances the ion communication of the fluid medium, resulting in the strong carbonate cementation throughout the whole thin sand body. The third type is the favorable reservoir in the exploration area, which holds the characteristics of a thick single layer sand body with less developed fracture and weak carbonate cementation only developed in the top and bottom surface of the sand body (Figure 9c). It is obvious that the third development pattern of carbonate cementation is a high-quality reservoir, that is, exploration target, and it is mainly controlled by sedimentary factors, which is manifested as relatively thick underwater distributary channel sand body. The effect of ion exchange of geological fluids and de-acidification of organic acids is relatively limited.

6 Conclusion

(1) The Chang 6 tight sandstone reservoir in the WJY area develops the slowly progradational underwater distributary channel sand body, which has the features of good plane continuity, poor vertical continuity, and thin single-layer thickness. Ferrocalcite is the main carbonate cement type that exists in porphyritic and crystal stock.
(2) Both carbonate cements and calcite veins hold similar diagenetic conditions. The dissolution of feldspar (mainly plagioclase) is the main calcium source. The de-acidification of organic acids is the main carbon source. The diagenetic stage is identified as the Mesogenetic A stage. The sedimentary environment has a low salinity, and the carbonate cements are formed in the condition of fresh and brackish water.
(3) The development model of Chang 6 carbonate cementation can be classified in three patterns: "eggshell pattern," "cutting pattern," and "favorable reservoir pattern," in which the "favorable reservoir pattern" with relatively thick single layer sand body, less fracture, and weak carbonate cementation is the favorable target in exploration and exploitation. The development degree of carbonate cementation significantly affects the physical properties of the reservoir.

Acknowledgments: This study was jointly supported by funds from the National Natural Science Foundation of China (Grant No. 41772142; 41802160).

References

[1] Bloch S, Lander RH, Bonnell L. Anomalously high porosity and permeability in deeply buried sandstone reservoirs: origin and predictability. AAPG Bull. 2002;86(2):301–28.
[2] Zhang S, Lu P. Effect of micrite content on calcite cementation in an upper jurassic carbonate reservoir, Eastern Saudi Arabia. J Petrol Geol. 2019;42(1):79–89.
[3] Oluwadebi AG, Taylor KG, Dowey PJ. Diagenetic controls on the reservoir quality of the tight gas Collyhurst Sandstone Formation, Lower Permian, East Irish Sea Basin, United Kingdom. Sediment Geol. 2018;371:55–74.
[4] Meshri ID. On the reactivity of carbonic and organic acids and generation of secondary porosity. In: Gautier DL, editor. Roles of organic matter in mineral diagenesis. SEPM Special Publication. 1986;38. p. 123–8.
[5] Xi KL, Cao YC, Jahren J, Zhu RK, Bjorlykke K, Haile BG, et al. Diagenesis and reservoir quality of the Lower Cretaceous Quantou Formation tight sandstones in the southern Songliao Basin, China. Sediment Geol. 2015;330:90–107.
[6] Dou W, Liu L, Wu K, Xu Z, Liu X, Feng X. Diagenetic heterogeneity, pore throats characteristic and their effects on reservoir quality of the Upper Triassic tight sandstones of Yanchang Formation in Ordos Basin, China. Marine Petrol Geol. 2018;98:243–57.
[7] Xiaoping Y, Wenzhi Z, Caineng Z, Mengjin C, Yanru G. Origin of low-permeability reservoir and distribution of favorable reservoir. Acta Petrol Sin. 2007;28(4):57.
[8] Tamar-Agha M. The influence of cementation on the reservoir quality of the Risha Sandstone Member (Upper Ordovician), Risha Gasfield, NE Jordan. J Petrol Geol. 2009;32(2):193–208.
[9] Tian Y, Shi Z, Song J, Wu X, Gao X. Diagenesis characteristics of the Chang 8-Chang 6 member of Yanchang Formation In Yichuan – Xunyi Area, Ordos Basin. J Southwest Petrol Univ (Sci Technol Ed). 2011;33(4):44–52.
[10] Taylor KG, Gawthorpe RL, Curtis CD, Marshall JD, Awwiller DN. Carbonate cementation in a sequence-stratigraphic framework: upper Cretaceous sandstones, Book Cliffs, Utah-Colorado. J Sediment Res. 2000;70(2):360–72.
[11] Zhixue S, Zhilei S, Hongjiang L, Xijie Y. Characteristics of carbonate cements in sandstone reservoirs: a case from Yanchang Formation, middle and southern Ordos Basin, China. Petrol Explorat Dev. 2010;37(5):543–51.
[12] Liu C, Zheng H, Hu Z, Yin W, Li S. Characteristics of carbonate cementation in clastic rocks from the Chang 6 sandbody of Yanchang Formation, southern Ordos Basin. Sci China Earth Sci. 2012;55(1):58–66.
[13] Tian Y, Shi Z, Li T, Liang X, Xin H, Wu X, et al. Characteristics and origin of the carbonate cements of Chang 8 member in Jiyuan area, Ordos Basin. J Xi'an Shiyou Univ (Nat Sci Ed). 2011;26(3):26–31.
[14] Wang Y, Liu L, Li S, Ji H, Xu Z, Luo Z, et al. The forming mechanism and process of tight oil sand reservoirs: a case study of Chang 8 oil layers of the Upper Triassic Yanchang formation in the Western Jiyuan Area of the Ordos Basin, China. J Pet Sci Eng. 2017;158:29–46.
[15] Wang L, Li W, Lin T, Wang R. Diagenesis and its influencing factors of the Chang 6 interval of Upper Triassic Yanchang Formation in Ordos Basin. J Palaeogeograph. 2012;14(3):311–20.
[16] Fanhao G, Zhidong BAO, Hancheng JI, Zhengping FAN, Li LIU, Xing WU. Study on the reservoir diagenesis heterogeneity of Chang 6 Member of Upper Triassic in Jiyuan Area of Ordos Basin. J Jilin Univ Earth Sci Ed. 2011;41(3):639–46.
[17] Kang Y, Chang-Zheng LI. Study on diagenesis differences of Chang 6 Stratum of Yangchang Formation in Ordos Basin. Ground Water. 2015;37(3):193–5.
[18] Irwin H, Curtis C, Coleman M. Isotopic evidence for source of diagenetic carbonates formed during burial of organic-rich sediments. Nature. 1977;269(5625):209–13.

[19] Wang D, Song W. Carbon isotope fluctuation in sediments: the potential tracer for generation of biogenic gas. Petrol Explorat Dev. 1992;19:47–51.
[20] Li Y, Zhang W, Li S, Luo A, Mou W, Deng X, et al. Characteristics of carbonate cements and their effects on properties in Chang 8 Sandstone Reservoir, Ordos Basin. Geol Sci Techol Inf. 2018;37(4):175–83.
[21] Guo RL, Xie QC, Qu XF, Chu MJ, Li ST, Ma DX, et al. Fractal characteristics of pore-throat structure and permeability estimation of tight sandstone reservoirs: a case study of Chang 7 of the Upper Triassic Yanchang Formation in Longdong area, Ordos Basin, China. J Pet Sci Eng. 2020;184:13.
[22] Yang Y, Li W, Ma L. Tectonic and stratigraphic controls of hydrocarbon systems in the Ordos basin: a multicycle cratonic basin in central China. AAPG Bull. 2005;89(2):255–69.
[23] Yao S, Zhang K, Hu W, Fang H, Jiao K. Sedimentary organic facies of the Triassic Yanchang Formation in the Ordos Basin. Oil Gas Geol. 2009;30(1):74.
[24] Mou W, Li S, Yan C. Genesis model of sandbodies in Chang 6 tight oil reservoirs in the Western Area of Jiyuan, the Ordos Basin. Spec Oil Gas Reserv. 2017;24:6–11.
[25] Guo R, Chen X, Ma X, Ma J, Wang Q, Chen L. Analysis of the characteristics and its influencing factors of horizontal movable fluid in the Chang 7 tight reservoir in Longdong area, Ordos basin. Nat Gas Geosci. 2018;29(5):665–74.
[26] Yao J, Wang Q, Zhang R, Li S. Forming mechanism and their environmental implications of chlorite-coatings in Chang 6 sandstone (upper Triassic) of Hua-Qing area, Ordos Basin. Acta Sedimentol Sin. 2011;29(1):72–9.
[27] Lai J, Wang GW, Chen J, Wang SC, Zhou ZL, Fan XQ. Origin and distribution of carbonate cement in tight sandstones: the upper Triassic Yanchang Formation Chang 8 oil layer in West Ordos Basin, China. Geofluids. 2017;13:8681753.
[28] Clark ID. Groundwater geochemistry and isotopes. Boca Raton, FL, USA: CRC Press; 2015.
[29] Longstaffe FJ. Clays and the Resource Geologist: A Short Course Sponsored by the Mineralogical Association of Canada and Held Immediately Following Their 1981 Annual Meeting at the University of Calgary, Calgary, Alberta, May 14th–16th, 7. Mineralogical Association of Canada; 1981.
[30] Ketzer JM, Holz M, Morad S, Al-Aasm I. Sequence stratigraphic distribution of diagenetic alterations in coal-bearing, paralic sandstones: evidence from the Rio Bonito Formation (early Permian), southern Brazil. Sedimentology. 2003;50(5):855–77.
[31] Shackleton NJ. Paleotemperature history of the Cenozoic and the initiation of Antarctic glaciation: oxygen and carbon isotope analyses in DSDP Sites 277, 279, and 281. Initial eports of Deep Sea Drilling Project. 1975;29: 743–56.
[32] Keith M, Weber J. Isotopic composition and environmental classification of selected limestones and fossils. Geochim Cosmochim Acta. 1964;28:1787–816.